Strain field measurements and simulation of dislocation propagation for nanoscale hardening precipitation

Patricia Donnadieu [1] —Guy F. Dirras[2] — Joël Douin[3]

[1)] *Laboratoire de Thermodynamique et Physico-Chimie Métallurgique, ENSEEG, CNRS / INPG*
Domaine Universitaire, BP 75, F38402 St Martin d'Hères
Tél.33(0)4 76 82 66 86 / Fax. : 33(0) 4 76 82 66 44/ E-mail : donnadie@ltpcm.inpg.fr

[2)] *Laboratoire de LPMTM-CNRS, Institut Galilée, / Université Paris XIII*
Av. J.B. Clément -F93193 Villetaneuse
Tél.33(0)1 49 40 34 88 / Fax. : 33(0)1 49 40 39 38 / E-mail : dirras@galilee.univ-paris13.fr

[3)] *Laboratoire d'Etudes des Microstructures, CNRS/ONERA,*
29 av. Division Leclerc, F92322 Châtillon
Tél.33(0)1 46 73 44 42 / Fax. : 33(0)1 46 73 41 55 / E-mail : douin@onera.fr

ABSTRACT. Hardening in Al alloys frequently results from the modification of dislocation propagation by a large density of nanometric precipitates. To study the precipitate/dislocation interaction in Al-Mg-Si alloys, we have carried out a TEM study of deformed samples complemented by a new approach combining image analysis and simulation of dislocation motion. The analysis of HRTEM image allows to measure the strain field which is further introduced in the simulation of the dislocation propagation. In the Al-Mg-Si alloy, the simulation indicates that dislocation motion in the matrix occurs by circumventing the rod shaped precipitates through activation of the Orowan process while the lath shaped precipitates can be sheared. This is in agreement with the observation of dislocation loops and traces of shear of the lath precipitates in deformed samples.

KEYWORDS precipitation hardening, Al-Mg-Si alloys, TEM, dislocation, precipitate strain field

1. Introduction

Nanoscale precipitation is frequently responsible for strengthening in materials such as Aluminum alloys. The microstructure typical of hardening is a large dispersion of nanometric precipitates. Actually the hardening effects (both hardening rate and yield strength increase) result from the interaction of dislocations with the nanoscale precipitates which act as obstacles to the dislocation motion. Basically the dislocations are pinned by the precipitates; under the increasing applied stress they will finally shear or by-pass the obstacles. As dislocations are moving in the matrix, their propagation, and hence the interaction mechanisms, are influenced by the strain field due to the precipitates. This strain field depends on precipitate characteristics: morphology, size, structure, composition and orientation relationships with the matrix. Most of these parameters are unknown since the hardening precipitates usually do not belong to the phase diagram.

Direct study of dislocation/precipitate interaction can be extremely difficult for microstructures presenting a dense dispersion of nanoscale precipitates. Therefore we propose an alternative approach: image analysis combined to the simulation of dislocation propagation. On the one hand, the phase image method, proposed by Hytch *et al.* (1997), allows extracting quantitative information on displacements from high resolution transmission electron microscopy (HRTEM) images. On the other hand the simulation of the dislocation propagation allows to predict the interaction mechanisms in the precipitate strain field.

The combination of image analysis and simulation provide then a tool to examine the dislocation behaviour when approaching the precipitates. Such tool is particularly appropriate to our case since no hypothesis on the structure composition nor the elastic properties of precipitates has to be used, the strain field created by the precipitates being the experimental one given by direct measurement. Besides, observation of deformed samples carried out in order to test the simulation results will be also reported. The system chosen as model case here is a Al-Mg-Si alloy (6XXX series) at peak hardening (T6 state). In this state, a large density of precipitates is observed: 10^{15} –10^{17} particles /cm^3 depending on solute contents. The precipitates shows two morphologies: laths and rods, the typical size are $\Phi \sim 5$ nm, L ~ 50 nm for rods and, L ~ 100 nm, l ~ 10 nm, e ~ 5 nm for laths.

2. Measurements of strain field from HRTEM images

The geometrical phase method (Hytch *et al.*, 1997) can be summarized as follows. The image of a crystalline area is decomposable in a set of periodic components g. In a perfect lattice, the phase of a g-component is constant, while in a lattice distorted by a displacement field u(x,y), the phase is $-2\pi g.u(x,y)$. In each point of the phase map, the intensity is proportional to u(x,y), the scaling factor is simply the grey level full range for a fringe spacing. The phase image method is able to detect very small strain field. Therefore, before using the method such as in the present simulation, its possibilities and limits for the extraction of strain field of nanoscale precipitates have been examined in details (Donnadieu *et al.*, 2001).

The HRTEM image in figure 1 shows a lath shaped precipitate in a 6056-T6 Al alloy, the longest lath dimension being parallel to the beam axis. Fig. 1b and 1c are the phase images for two Fourier components g1 and g2 selected from the FFT of the area (insert in Fig. 1). Since g1 and g2 are not collinear, the phase map allows for a complete determination of the displacement field in the image plane but no information on the component perpendicular to the image. However, for elongated precipitates, and this is hopefully the case in 6XXX-T6 Al alloys, the displacement field is very small, if not zero, along this elongation direction.

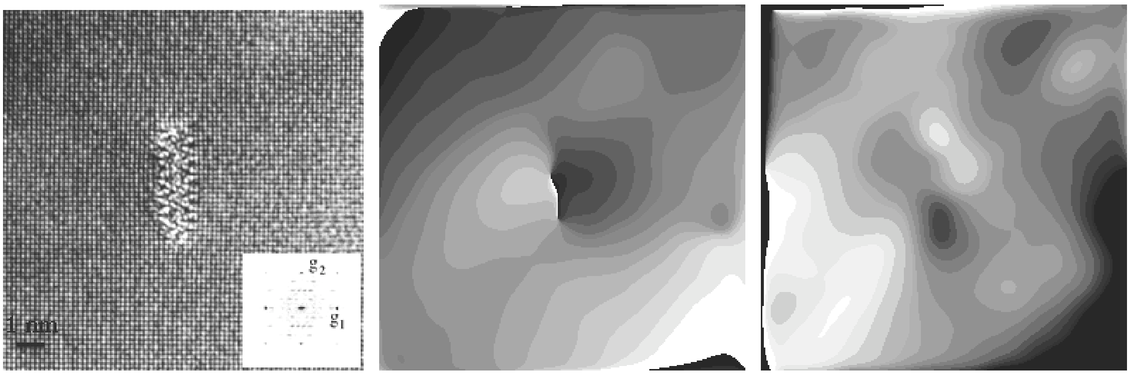

(a) (b) (c)

Figure 1. a) HRTEM image of a lath precipitate embedded in the Al matrix (6056-T6 alloy) b) Phase map obtained with the g1 selected vector c) Phase map obtained with the g2 selected vector

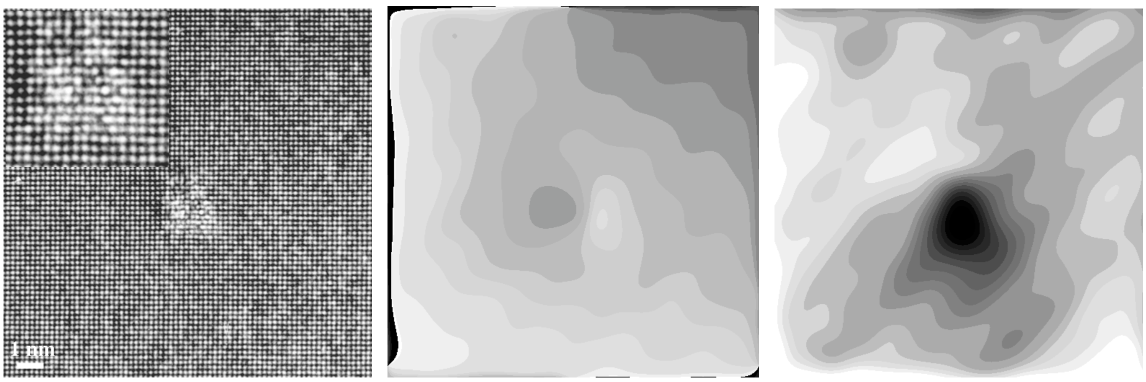

(a) (b) (c)

Figure 2. a) HRTEM image of a rod precipitate embedded in the Al matrix (6056-T6 alloy). b) Phase map obtained for a g1 direction c) Phase map obtained for the g2 direction.

Figure 2a is a HRTEM image of a rod precipitate seen edge on. As illustrated by the insert, the precipitate structure is quite ill-defined and the matrix is highly deformed by the rod precipitate. Fig. 2b and 2c are the related deformation maps. Fig. 2c clearly shows the asymmetry of the displacement field due to the rod. The stress field is obtained by derivation of phase maps and using the matrix elastic constant. The interaction of dislocations with lath or rod can be then specifically addressed.

3. Simulation of dislocation propagation in the experimental strain field

The simulation used here is based on the equations of the dynamics of dislocations, including short-range and long-range interactions. It also allows any dislocation character, as earlier developed by Bacon (1967). In the simulation, the dislocation moves under the applied stress, the line tension as well as the measured stress field due to the precipitate. Figure 3 shows the simulated movement of a dislocation in the vicinity of a rod or of a lath under the same applied stress. For the rod, the stress acting on the dislocation is not sufficient for the dislocation to attain the precipitate, the rod can then only be by-passed by formation of a dislocation loop, the so-called Orowan process. In the case of a lath, as the residual stress is smaller than around a rod, the dislocation is not stopped by the surrounding stress field and can shear the precipitate.

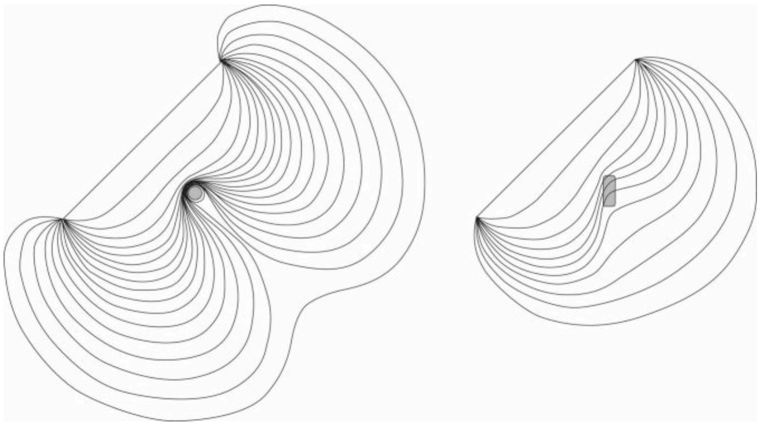

(a) (b)

Figure 3. Comparison of the simulated movements of a 1/2<110> dislocation under a constant applied stress in the vicinity of a rod (a) or of a lath (b). The dislocation has been drawn for successive positions corresponding to a constant interval of time, identical for both simulations. Notice that the shearing of the lath starts at the small end of the lath, which corresponds to the lowest stressed area of the matrix near the surface of the lath.

Here, to simplify the simulation of the shearing of the lath, two assumptions were made, both justified by the small cross section of the lath: (i) as the crystallography of the precipitate is unknown, we assume no change in Burgers vector of the dislocation nor glide plane while shearing, and (ii) the stress field inside the precipitate has been taken constant and equal to the stress at the interface between matrix and precipitate. These two assumptions are not very important since the simulation main result is that the residual stress is not sufficient to prevent the dislocation to attain the interface of a lath precipitate. The simulation shows that the stress field around laths, relatively small compared to the rod case, appears to be at the origin of a difference on the dislocation behaviour.

4. TEM study of deformed 6061 alloys

Because of the high density of precipitates, no clear good observations of dislocations can be made on the 6056 Al alloys studied above by HRTEM. Since in Al-Mg-Si alloys, and depending on the solute content, the precipitate density can vary from an alloy to another for similar precipitate size, we have chosen an alloy showing a smaller precipitate density, namely a 6061 alloy in the T6 state. Samples were compression tested up to 2% engineering deformation at room temperature (strain rate of 10^{-4} s^{-1}). TEM observations were carried out under dark field conditions. The weak beam dark field image in Fig. 4a shows the overall dislocation structure following 2% deformation: dislocations are extensively pinned all along by precipitates making it difficult for them to move as it can be seen by numerous bowing out segments. The striking feature here is the high density of small and elongated dislocation loops just as large as the rod-like precipitates. This observation suggests that dislocations actually bypass precipitates through an Orowan like process.

Larger loops and dislocation dipoles were also profusely seen. As for the possibility of precipitate shearing, the imaging conditions did not allow to visualise dislocation and the precipitates in the same time. Nonetheless, high magnification weak beam studies were carried out to investigate the structure of the precipitate after straining (Fig.4b). As illustrated by the insert in Fig. 4b, some laths exhibit traces of shearing after deformation.

The rate at which precipitate shearing occurs and the quantification of the mechanism was not investigated. Nevertheless, we do think that it occurs only locally compared to the bypassing process. Because of their small size and pseudo coherency, the precipitates are expected to be sheared by dislocations. However, in situ experiments or post mortem analysis did not directly show such a mechanism (Gehanno, 1995; Vivas, 1997; Vivas *et al.*, 1997). The actual observation of extensive dislocations bypassing precipitates as the major mechanism is in agreement with the results of the simulation indicating shearing of lath and by passing for rods.

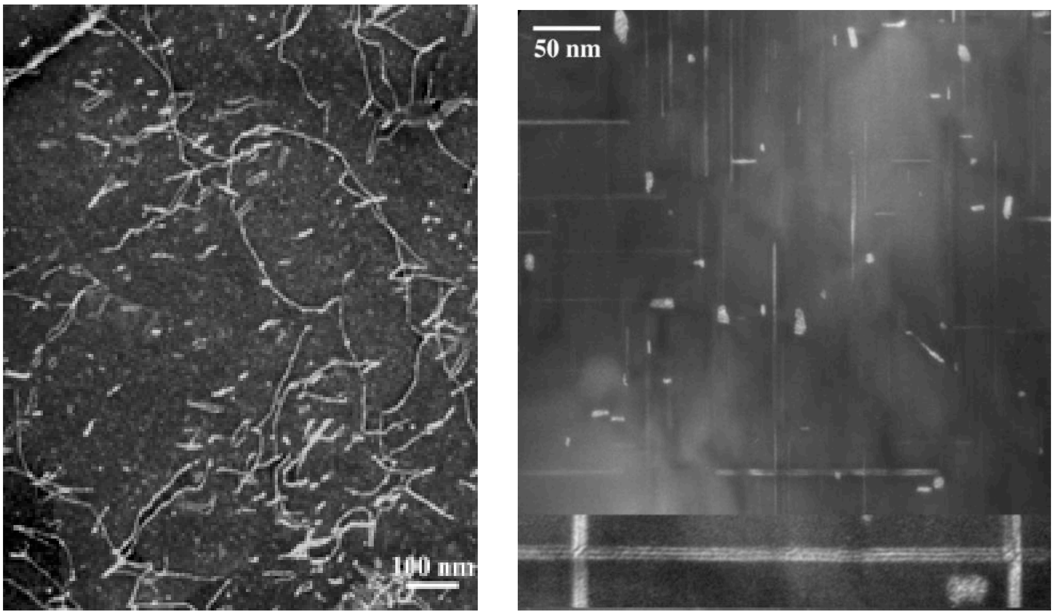

(a) (b)

Figure 4. a) Weak beam images of the deformed 6061-T6 alloy. Note the numerous small elliptical loops. b) Traces of laths and rods imaged by dark field taken along the [100] zone axis in the deformed sample. Some laths show traces of shearing (see insert at the bottom of Fig. 4b at glancing angle)

5. Summary

Deformation mechanisms for hardening precipitation are particularly difficult to study because of the density, scale and complex morphology of the precipitates with metastable unidentified phases. Using HRTEM image analysis and simulation of dislocation propagation, we have analysed the impact of the precipitate strain field on the mechanisms. It comes out that the strain field is responsible for the by passing of the rod while the shearing of lath is allowed. TEM observations of deformed samples have confirmed the simulation predictions. According to these first results, the combination of HRTEM to simulation of dislocation propagation appears as an appropriate method to overcome the complexity arising from a too fine scale microstructure.

Bacon D. J., *Physic Status Solidi*, 23, 1967, p. 527

Donnadieu P., Matsuda K., Epicier T., Douin J., « Measurements of strain fields due to nanoscale precipitates using the phase image method », *Image Analysis and Stereology*, vol. 20, n°3, 2001, pp 213 –218

Gehanno H., "Comportement à chaud d'alliage Al-Si-Mg" Thèse de doctorat, Institut National Polytechnique de Grenoble, 1995

Hytch M. J., Snoeck E., Kilaas R., "Quantitative measurements of displacement and strain fields from HREM micrographs", *Ultramicroscopy*, vol 74, 1998, p.131-146

Vivas M., "Etude par microscopie électronqiue de la microstrucuture et des mécanismes de déformation de l'alliage d'aluminium 6056", Thèse de Doctorat, University of Toulouse, 1997

Vivas M., Lours P., Levaillant C., Couret A., Casanove M.J., Coujou A., "Determination of precipitate strength in aluminium alloy 6056-T6 from transmission electron microscopy in situ straining data", *Phil. Mag. A*, vol. 76, n°5, 1997, 921-931